Supporting Information

Formation of Hollow MoS_2/Carbon Microspheres for High Capacity and High Rate Reversible Alkali-Ion Storage

Tianyu Yang,[a, b‡] Ji Liang,[c‡] Irin Sultana,[a] Md Mokhlesur Rahman,[a] Michael J. Monteiro,[b] Ying (Ian) Chen,[a] Zongping Shao,[d,e]* S. Ravi P. Silva[f] and Jian Liu[b,e,f,g]**

[a] Institute for Frontier Materials, Deakin University, Geelong, VIC 3216, Australia

[b] Australian Institute for Bioengineering and Nanotechnology, The University of Queensland, Brisbane, QLD 4072, Australia

[c] Institute for Superconducting & Electronic Materials, Australian Institute of Innovative Materials, University of Wollongong, Innovation Campus, Squires Way, North Wollongong, NSW 2500, Australia

[d] Jiangsu National Synergetic Innovation Center for Advanced Materials, College of Chemical Engineering, Nanjing Tech University, No.5 Xin Mofan Road, Nanjing, 210009, PR China

[e] Department of Chemical Engineering, Curtin University, Perth, WA 6845, Australia

[f] Advanced Technology Institute & Department of Chemical and Process Engineering, University of Surrey, Guildford, Surrey, GU2 7XH, UK

[g] State Key Laboratory of Catalysis, Dalian Institute of Chemical Physics, Chinese Academy of Sciences, 457 Zhongshan Road, Dalian 116023, China

* Addresses correspondence to: jian.liu@surrey.ac.uk; zongping.shao@curtin.edu.au; ian.chen@deakin.edu.au

‡ These authors contributed equally to this work.

Keywords: molybdenum disulfide, carbon nanosphere, hollow microspheres, lithium ion battery, sodium ion battery

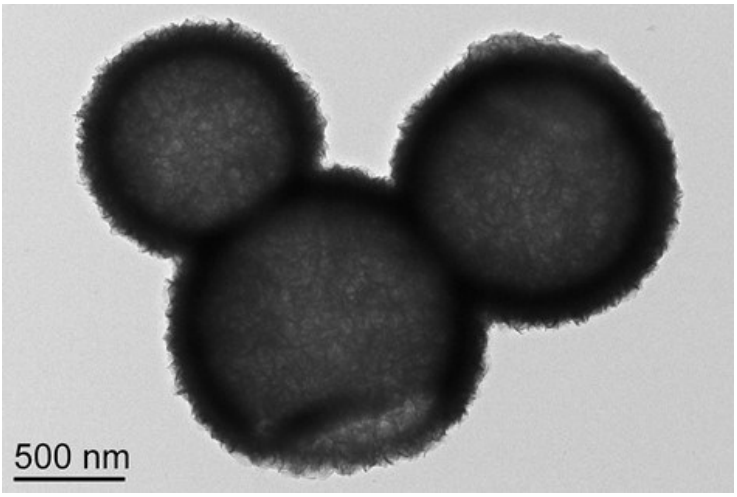

Figure S1. The TEM image of RF@MoS_2.

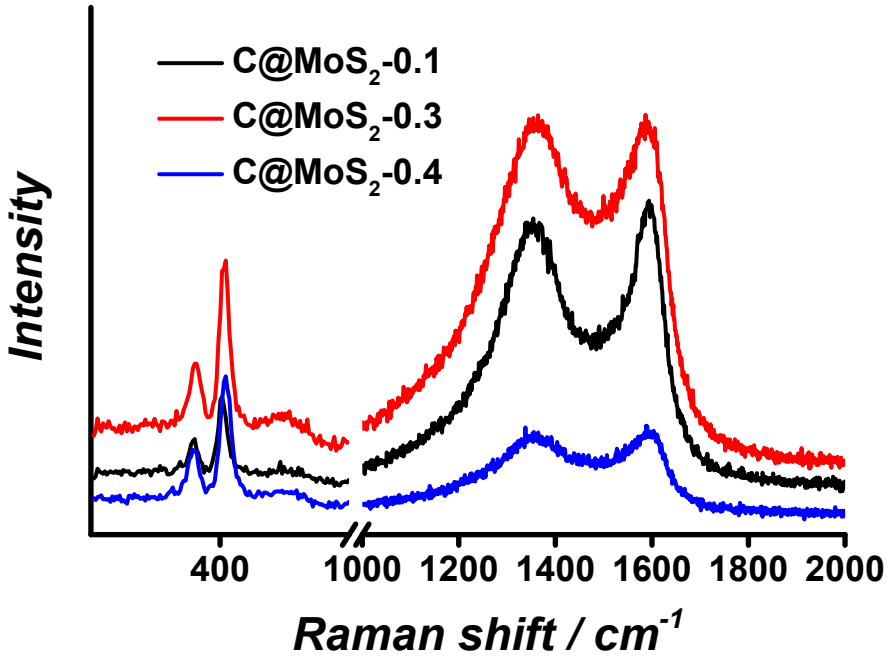

Figure S2. The Raman spectra of the samples.

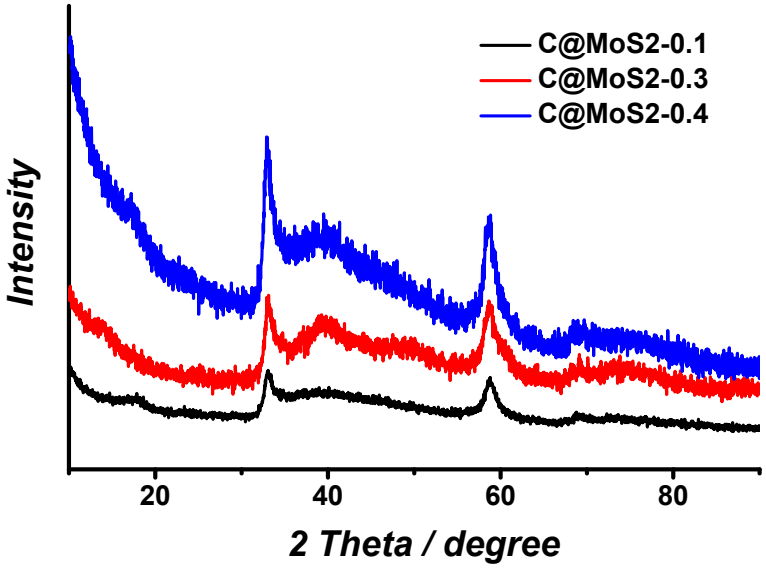

Figure S3. The XRD spectra of the samples.

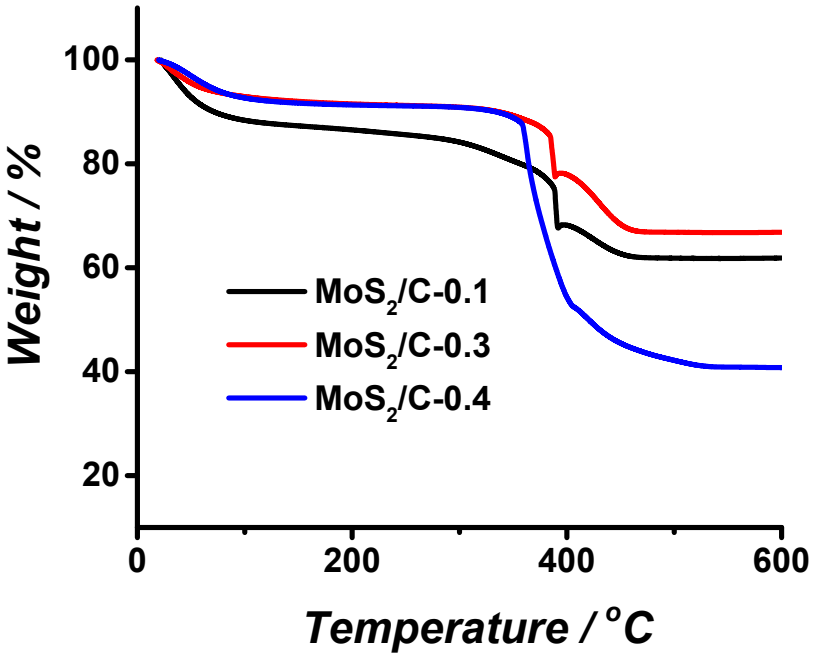

Figure S4. The thermogravimetric analysis of the samples.

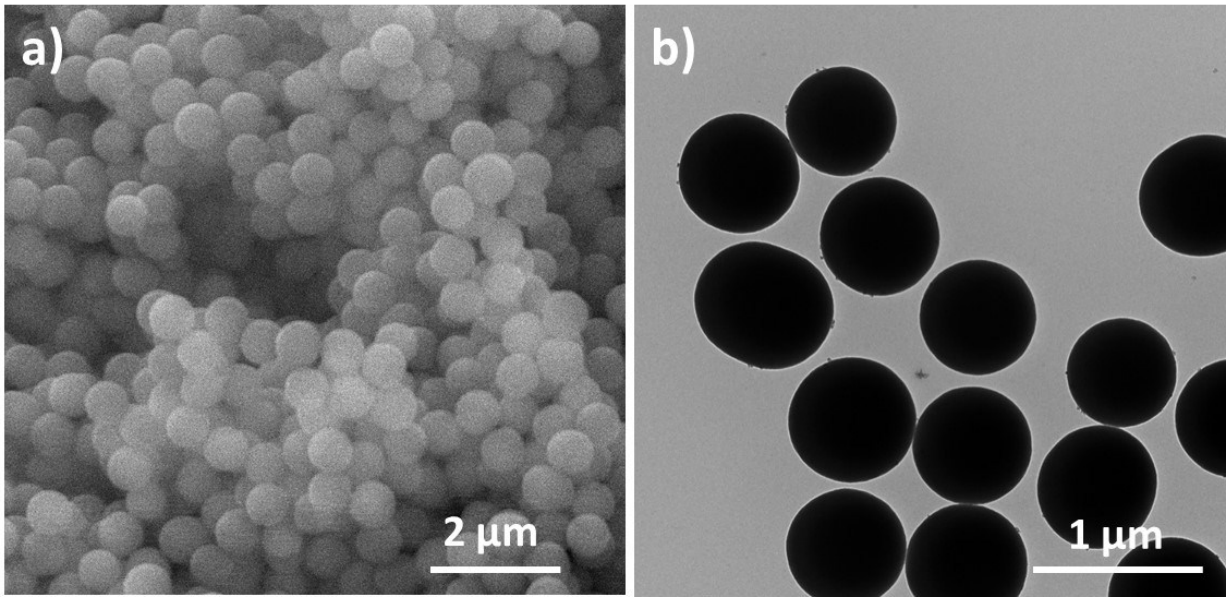

Figure S5. a) SEM and b) TEM images of the polymer spheres prepared without adding Na_2MoO_4 in the system. All other precursors and experimental parameters are the same.

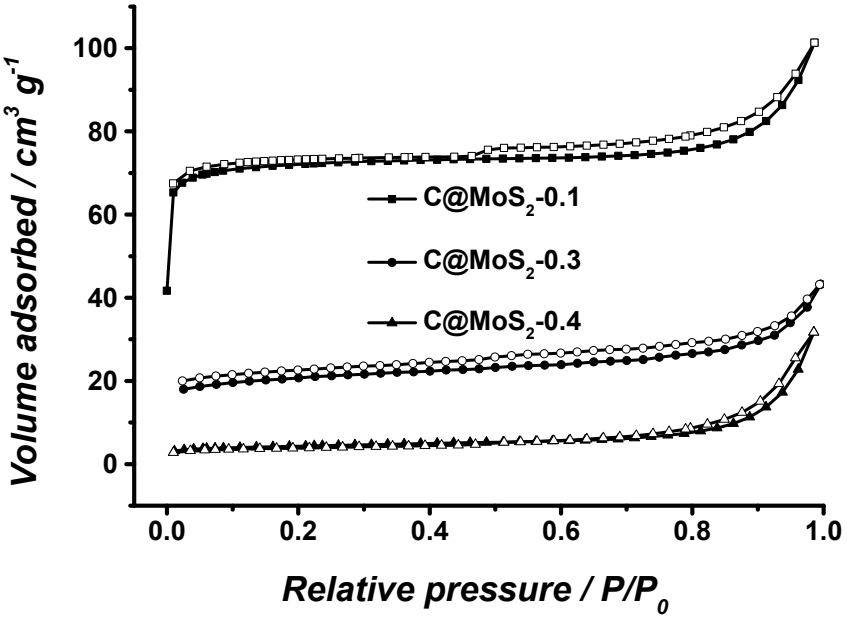

Figure S6. The nitrogen adsorption-desorption isotherms of the samples.

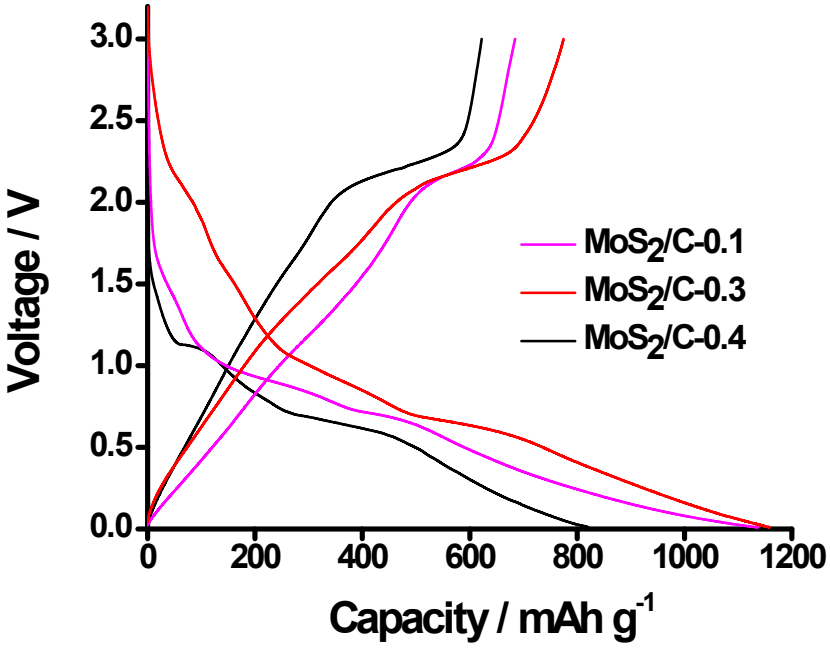

Figure S7. The first charge-discharge profiles of the samples.

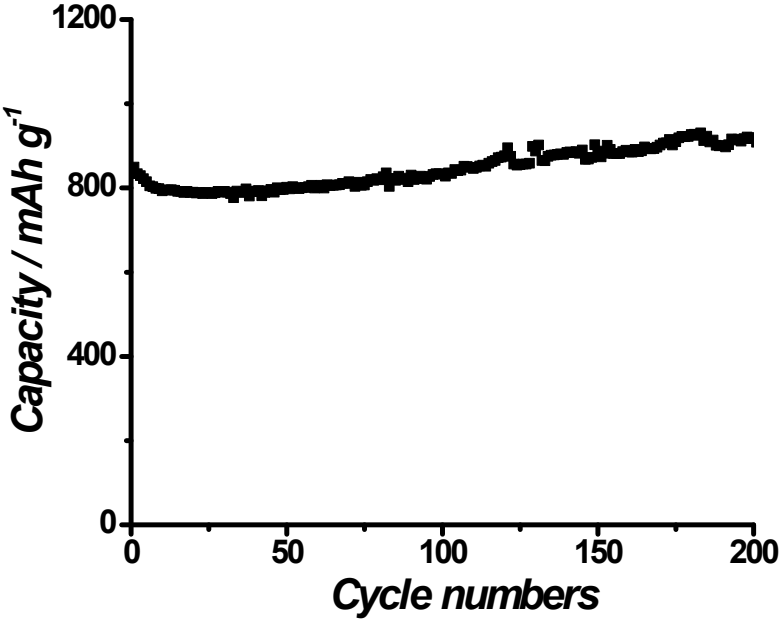

Figure S8. The cycling stability of MoS_2/C-0.3 sample tested for 200 cycles.

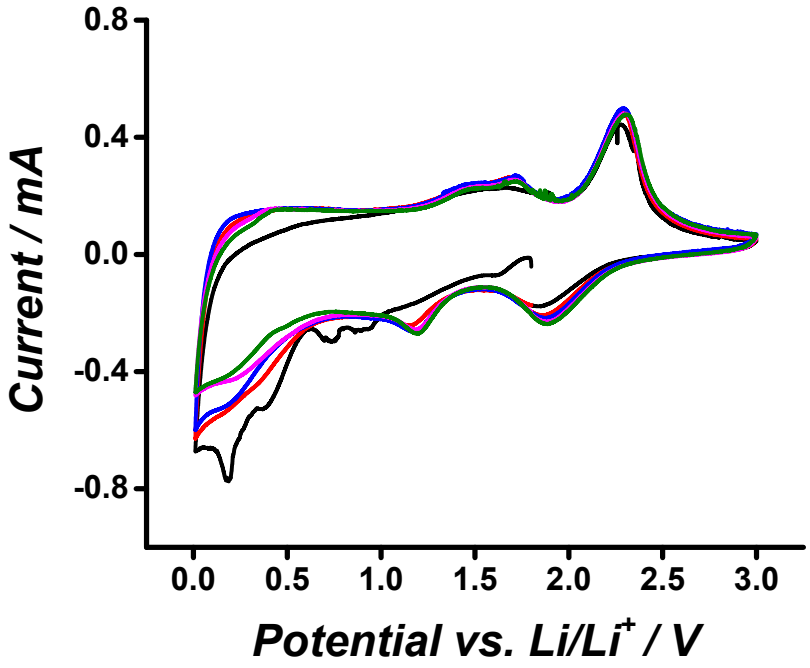

Figure S9. The LIB cyclic voltammetry profile of MoS_2/C-0.3 sample.

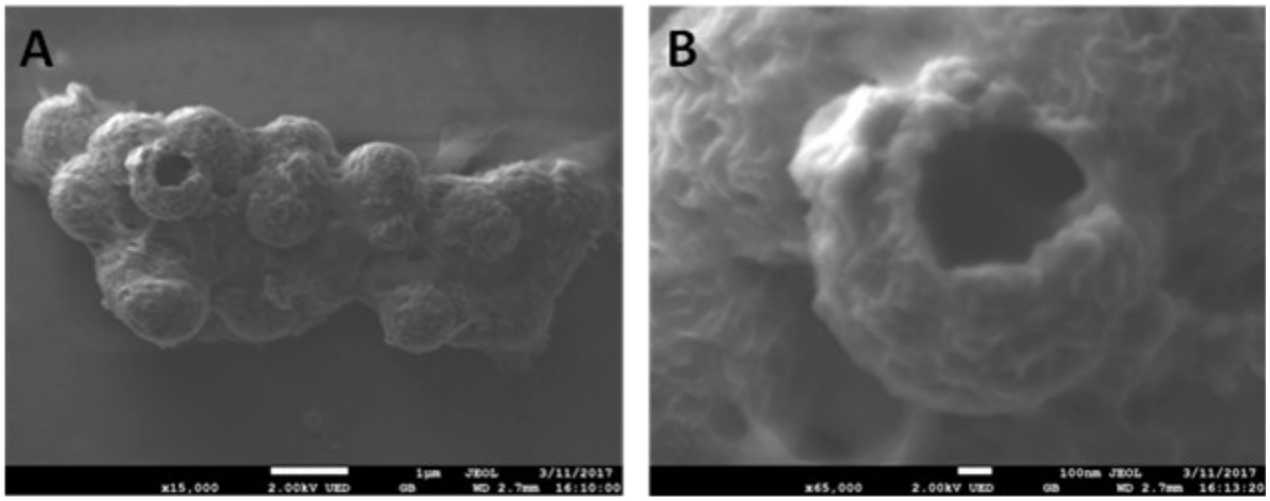

Figure S10. The a) SEM image and b) HRSEM image of MoS_2/C-0.3 sample after first charge.

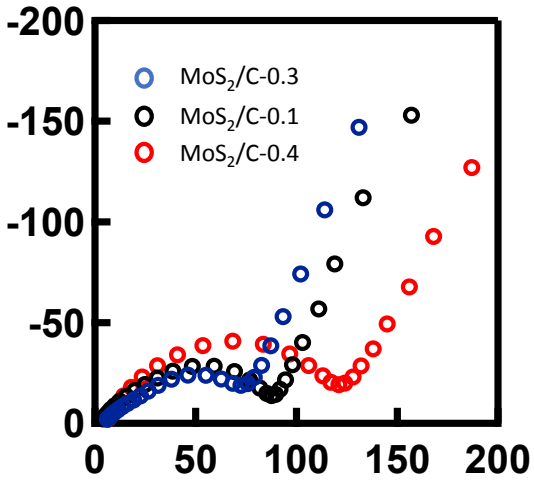

Figure S11. The EIS after the first cycle of the MoS_2/C-0.3, MoS_2/C-0.1 and MoS_2/C-0.4 samples.

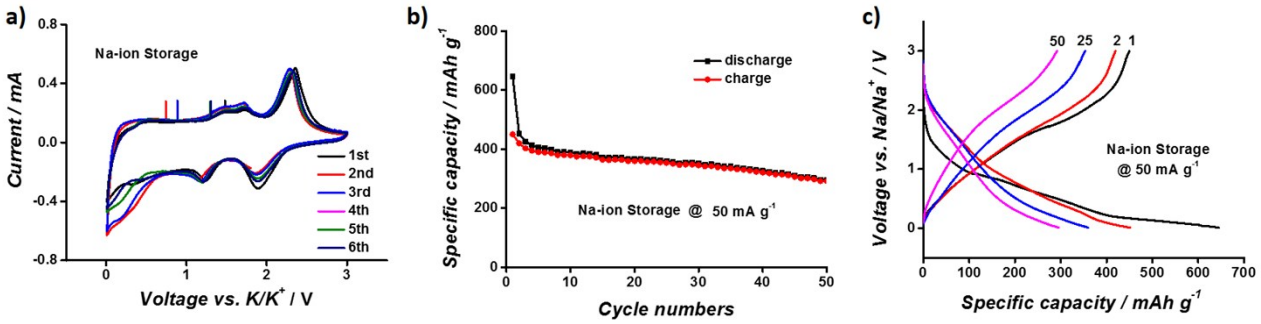

Figure S12. The Sodium ion battery evaluation profile of the sample C@MoS_2-0.3, a) Cyclic Voltammograms (CV) Profile; b) Cycling stability; and c) Charge-discharge profile.

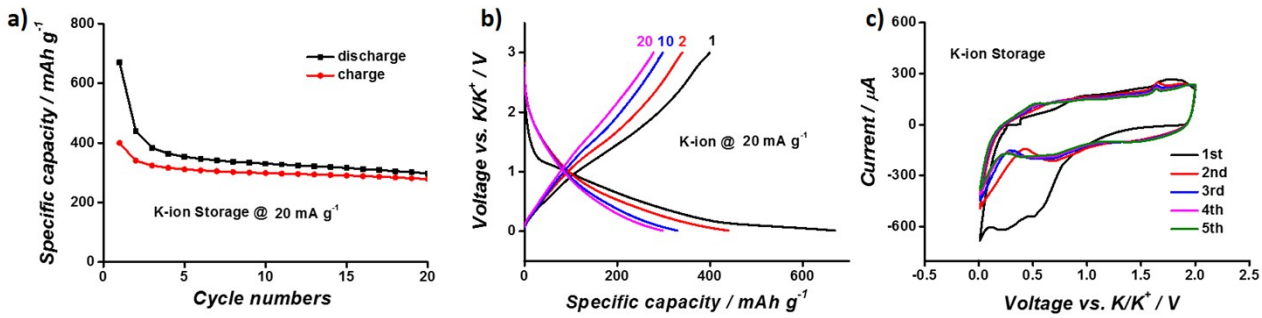

Figure S13. The Potassium ion battery evaluation profile of the sample C@MoS_2-0.3 including A) Cycling stability, B) Charge-discharge profile, C) Cyclic voltammograms (CV) Profile.

Table S1. Recent advances of LIB battery performance of MoS_2 electrodes

Types of materials	**Voltage Range [V]**	**Discharge capacity**	**Current density [mA g^{-1}]**	**Reference**
This work	0.1-3	917 mAh g^{-1} after 200 cycles	100	
Hierarchical MoS_2 nanotubes	0.1−3.1	727 mAh g^{-1} after 100 cycles	100	[1]
Single-layered MoS_2 assembled nanotubes	0.01−3	839 mAh g^{-1} after 50 cycles	100	[2]
Hierarchical MoS_2 microboxes	0.05−3	900 mAh g^{-1} after 50 cycles	100	[3]
Yolk-Shelled MoS_2 spheres	0.001−3	687 mAh g^{-1} after 100 cycles	1000	[4]
MoS_2 nanosheets on CNTs (1)	0.01−3	698 mAh g^{-1} after 60 cycles	100	[5]
MoS_2 nanosheets on CNTs (2)	0.01−3	823.4 mAh g^{-1} after 30 cycles	100	[6]
MoS_x/CNTs ($2 < x < 3$)	0.01−3	≈1000 mAh g^{-1} after 30 cycles	50	[7]
MoS_2 nanosheets on N-doped carbon nanoboxes	0.005−3	952 mAh g^{-1} after 200 cycles	400	[8]
MoS_2 nanosheets on carbon nanospheres	0.01-3	802 mAh g^{-1} after 50 cycles	50	[9]

Table S2. Recent advances of SIB battery performance of MoS_2 electrodes

Types of materials	**Voltage Range [V]**	**Cycling Performance**	**Rate Performance**	**Reference**
		Capacity [mA h g^{-1}]/Cycles/Current Density [mA g^{-1}]	**Capacity [mA h g^{-1}]/Current Density [A g^{-1}]**	
This work	0.01-3	291/50/50	200/1000	
MoS_2 ultrathin nanosheet	0.4-3	386/40/100	305/320	[10]
MoS_2 nanoflower	0.01-3	300/1000/1500	175/10,000	[11]
3D flower-like MoS_2/C nanosphere	0.01-3	520/67/50	390/1340	[12]
MoS_2/graphene 3D microspheres		323/1500/600	80/10,000	[13]
MoS_2 on Carbon Papers		286/80/100	205/1000	[14]
MoS_2 on graphene		254/80/300	352/640	[15]

Table S3. Recent advances of PIB battery performance of MoS_2 electrodes

Types of materials	**Reversible Capacity [mA h g^{-1}]**	**Cycling Performance**	**Reference**
		Capacity [mA h g^{-1}]/Cycles/Current Density [mA g^{-1}]	
This work	399	278/20/20	
Graphite	244	200/50	[16]
Soft carbon	214	170/50/2000	[17]
F doped Graphene	356	165/200/500	[18]
Sn/C	150	110/30/25	[19]
Sb/C	250	250/40/35	[20]

[1] G. Li, X. Zeng, T. Zhang, W. Ma, W. Li, M. Wang, CrystEngComm 2014, 16, 10754.
[2] P.-p. Wang, H. Sun, Y. Ji, W. Li, X. Wang, Advanced Materials 2014, 26, 964.
[3] L. Zhang, H. B. Wu, Y. Yan, X. Wang, X. W. Lou, Energy & Environmental Science 2014, 7, 3302.
[4] Y. N. Ko, Y. C. Kang, S. B. Park, Nanoscale 2014, 6, 4508.
[5] S. Ding, J. S. Chen, X. W. Lou, Chemistry – A European Journal 2011, 17, 13142.
[6] S.-K. Park, S.-H. Yu, S. Woo, B. Quan, D.-C. Lee, M. K. Kim, Y.-E. Sung, Y. Piao, Dalton Transactions 2013, 42, 2399.
[7] Y. Shi, Y. Wang, J. I. Wong, A. Y. S. Tan, C.-L. Hsu, L.-J. Li, Y.-C. Lu, H. Y. Yang, 2013, 3, 2169.
[8] X.-Y. Yu, H. Hu, Y. Wang, H. Chen, X. W. Lou, Angewandte Chemie International Edition 2015, 54, 7395.
[9] J. Jin, B. Kim, M. Kim, N. Park, S. Kang, S. M. Lee, H. J. Kim, S. U. Son, Nanoscale 2015, 7, 11280.
[10] D. Su, S. Dou, G. Wang, Advanced Energy Materials 2015, 5, 1401205.
[11] Z. Hu, L. Wang, K. Zhang, J. Wang, F. Cheng, Z. Tao, J. Chen, Angewandte Chemie 2014, 126, 13008.
[12] S. H. Choi, Y. N. Ko, J.-K. Lee, Y. C. Kang, Advanced Functional Materials 2015, 25, 1780.
[13] J. Wang, C. Luo, T. Gao, A. Langrock, A. C. Mignerey, C. Wang, Small 2015, 11, 473.
[14] X. Xie, T. Makaryan, M. Zhao, K. L. Van Aken, Y. Gogotsi, G. Wang, Advanced Energy Materials 2016, 6, 1502161.
[15] X. Xie, Z. Ao, D. Su, J. Zhang, G. Wang, Advanced Functional Materials 2015, 25, 1393.
[16] S. Komaba, T. Hasegawa, M. Dahbi, K. Kubota, Electrochemistry Communications 2015, 60, 172.
[17] Z. Jian, W. Luo, X. Ji, Journal of the American Chemical Society 2015, 137, 11566.
[18] Z. Ju, S. Zhang, Z. Xing, Q. Zhuang, Y. Qiang, Y. Qian, ACS Applied Materials & Interfaces 2016, 8, 20682.
[19] W. D. McCulloch, X. Ren, M. Yu, Z. Huang, Y. Wu, ACS Applied Materials & Interfaces 2015, 7, 26158.
[20] I. Sultana, T. Ramireddy, M. M. Rahman, Y. Chen, A. M. Glushenkov, Chemical Communications 2016, 52, 9279.